Case Studies in Construction Materials 16 (2022) e01102

Contents lists available at ScienceDirect

Case Studies in Construction Materials

journal homepage: www.elsevier.com/locate/cscm

Assessment of shear strength of reinforced concrete beams without shear reinforcement: A comparative study between codes of practice and artificial neural network

Thushara Jayasinghe *, Tharaka Gunawardena, Priyan Mendis

Faculty of Engineering and Information Technology, The University of Melbourne, Melbourne, Australia

ARTICLE INFO

Keywords:
Shear strength
Size effect
Strain effect
Back-propagation neural network
Sigmoid function

ABSTRACT

Despite 70 years of investigations in understanding the shear behaviour of reinforced concrete members, it is again gaining attention among structural engineers as the recently issued Australian concrete design standard, AS 3600 updated its shear provisions and ACI 318 unveiled its new one-way shear design equation. This study investigates the shear design equations in ACI 318–19 and AS 3600–2018 highlighting their strengths and weaknesses. A detailed parametric study is performed on a database of 1237 shear tests of point loaded RC slender beams without shear reinforcement. An Artificial neural network (ANN) was built, trained and validated with a subset of this database. Further, a very few experimental tests were conducted isolating the effect of a single variable on the shear failure load of RC beams without shear reinforcement. Thus, an ANN is an effective tool to investigate the influence of each variable individually. This study concludes that the introduction of size effect and $\rho_w{}^{1/3}$ terms into the new ACI 318–19 code have resulted in greater accuracy compared to ACI 318–14 which it replaced. The study further demonstrates that AS 3600–2018 agrees well with all ranges of test parameters. The ANN demonstrated more accurate predictions compared to the codes of practice within the range of input parameters considered.

1. Introduction

Shear failures are brittle in nature resulting in catastrophic failures with limited prior warning and no possibility of redistribution of internal stresses. Therefore, shear failures are naturally more dangerous and demand greater attention by structural engineers where structures need to be particularly designed to avoid sudden shear failures [1]. Shear failure of reinforced concrete beams is very complex in nature and are governed by several factors including shear span to depth ratio, longitudinal reinforcement ratio, member depth, crack width and presence or absence of transverse reinforcement. As a result, a simple, general and universally accepted shear prediction procedure has not yet been established. Therefore, some of the worldwide concrete design codes still rely on empirically derived shear design procedures.

During the last few decades, experimental investigations found that ACI 318–14 [2] shear provision inadequately predicted the shear response of large, lightly reinforced beams without shear reinforcement [1,3–9]. Thus, ACI 318–19 [10] has come up with a new one-way shear design equation addressing the major drawbacks of its predecessor ACI 318–14. An iterative procedure based on a

* Corresponding author.
E-mail address: tjayasinghe@student.unimelb.edu.au (T. Jayasinghe).

https://doi.org/10.1016/j.cscm.2022.e01102
Received 23 January 2022; Received in revised form 26 March 2022; Accepted 20 April 2022
Available online 22 April 2022

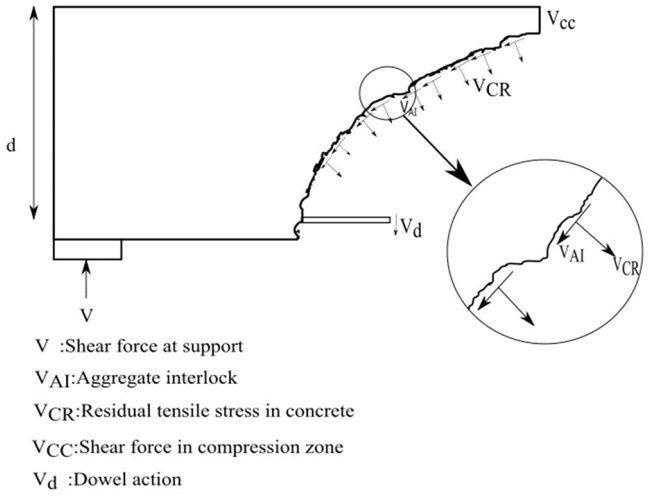

Fig. 1. Shear transfer mechanisms in reinforced concrete beam without shear reinforcement.

rational approach for shear was developed at the University of Toronto, and it is known as the "Modified Compression Field Theory" [11] which showed better agreement with a wide range of experimental results [12,13]. Subsequently, the simplified versions of Modified Compression Field Theory (MCFT) were developed and few concrete design codes including the Canadian concrete code [14], Fib model code [15], AASTHO LFRD [16] and AS 3600–2018 [17] adopted the Simplified Modified Compression Field Theory (SMCFT) [12] for the designing of RC beams without shear reinforcement. Later, several analytical formulations such as critical shear crack theory [18], critical shear displacement theory [19] and shear crack propagation theory [20] were developed to predict the failure shear strength of reinforced concrete beams without shear reinforcement.

The traditional modelling approaches in codes of practice in the form of empirical or analytical equations are mostly followed by a regression analysis using experimental data to determine unknown coefficients. However, the effectiveness of these equations is strongly affected by the datasets used for their calibration. Therefore, this study examines the capabilities of an artificial neural network (ANN) in predicting the shear failure strength of RC beams without shear reinforcement. ANN is a powerful tool to develop a relationship between given inputs and desired output. The architecture of an ANN composes of an input layer, hidden layers and output layers and the number of neurons in each layer must be determined from a trial-and-error analysis. Further, there are number of paradigms, but multi-layer back-propagation neural network is mostly used in analytical structural engineering research and also employed in this study.

In this study, the main parameters influencing sectional shear failures were briefly reviewed. Using a database of 1237 shear tests, the accuracy of the shear provisions in ACI 318–19 and AS 3600–2018 were reviewed. More importantly, new changes in the ACI 318–19 and AS 3600–2018 were evaluated against this database and their effectiveness in predicting the shear strength of beams without shear reinforcement was investigated. Further, an ANN model was developed using a subset of this database and strengths and weaknesses of the ANN were also discussed.

1.1. Research significance

This study collects the beam shear test data since 1950 and developed a database of 1237 beam tests without shear reinforcement. ACI 318–19 and AS 3600–2018 are recently updated their shear design provisions which performance of these provisions were not widely evaluated against a large dataset and against artificial neural network. Further, this study evaluates the accuracy several new terms added to ACI 318–19 which improved the shear strength predictions. Finally, a parametric study was performed using the trained ANN function in which the performances of these code equations were further evaluated.

1.2. Overview of shear behaviour of beams without shear reinforcement

A thorough understanding of the mechanism of shear behaviour of a flexurally cracked beam without shear reinforcement is crucial for design engineers to appreciate the vulnerability of their structures to shear failures. The shear span to depth ratio (a/d) is essentially a measure of the slenderness of the zones subjected to shear. Based on the shear span to depth, two different shear transfer mechanisms have been identified [21], namely, arch action in deep beams and beam action in slender beams. It was found that beam action is more critical than the arch action depending on the geometric properties of the beams. Initially, the total shear force would be carried by beam action. After failure of the beam action, redistribution of shear stress occurs allowing arch action to be activated. When arch action reaches its capacity, shear failure occurs in reinforced beams without shear reinforcement [3]. Beam action, which governs the failure of slender beams, depends on diagonal tensile stresses in the web of the member [22,23]. When the concrete in the web of a beam reaches its tensile capacity, diagonal tension cracks occur in a direction parallel to the principal compressive stress.

A shear stress that can be carried by a diagonally cracked RC beam relies on the shear transfer actions uncracked compression zone, aggregate interlock and dowel action [24], as shown in Fig. 1. Failure of at least one of the aforementioned mechanisms can lead to catastrophic shear failures. The capacity of the uncracked compression zone, which contributes to 20–40% of total shear strength at a cracked section [24], relies on the depth of the uncracked zone and the compressive strength of the concrete. Aggregate interlock, approximately 30–50% of the shear strength transferred through this mechanism [24], depends on aggregate size, concrete strength, longitudinal strain, crack width and the ductility of concrete relative to that of its aggregate. The remaining 15–25% will be carried by dowel action [24,25]. Once a diagonal crack reaches the level of longitudinal reinforcement bars, dowel forces are formed in the reinforcement to resist shear displacement due to crack propagation. The capacity of the dowel action is explicitly governed by the yield strength of longitudinal reinforcement, tensile strength of concrete and thickness of the cover. In terms of numerically predicting the above mechanisms, it is important to note that each mechanism depends on at least two or three parameters resulting in an intricate behaviour.

1.3. Principal variables affecting shear strength

I. Compressive strength of concrete ($f_c^{'}$)– The diagonal tensile capacity of concrete increases with increasing $f_c^{'}$. However, initially, Kani [6] concluded that the influence of $f_c^{'}$ on shear strength was insignificant and could be ignored in shear response estimations. Furthermore, for high strength concrete beams, a decreasing tendency of shear strength was revealed [26,27] and the fracture surfaces were considerably smooth [28], demonstrating that the shear force which is contributed by aggregate interlock decreases with increasing $f_c^{'}$. Angelakos et al. [4] presented load displacement behaviour of large beams with different concrete strengths and experienced no significant influence of $f_c^{'}$ on shear strength of beams.

II. Longitudinal reinforcement ratio (ρ_w) – The percentage of longitudinal reinforcement in a reinforced concrete beam has a crucial effect on its shear transfer mechanism. Elzanaty, et al. [29] explained that when the ρ_w is high, the penetration of the flexural crack in the compression zone is low resulting in an increase in the shear strength of the beam. Moreover, the greater the ρ_w, the narrower the cracks resulting in greater aggregate interlock contribution to shear resistance. Thus, as the ρ_w increases the shear strength of RC beams increase [30,31]. Angelakos, et al. [4,32] reported that changing ρ_w from 0.5% to 2.09% caused a 62% rise in the observed shear strength of large concrete beams.

III. Shear span to depth ratio (a/d) – It is effectively a measure of slenderness of the beams subjected to shear. As mentioned before, according to a/d ratio shear transfer mechanisms are two fold: beam action and arch action. Furthermore, the effect of a/d ratio on shear strength of RC beams were well documented in Hu & Wu [33] and it was found that the shear capacity of RC beams increased when a/d decreased. Longer specimens with higher a/d ratios were controlled by the breakdown of beam action while short beams failed due to the crushing of a concrete strut [3].

IV. Depth of beam (Size effect) – Another significant parameter that can affect the shear strength is the size of the specimen [7]. The size difference in beams will influence crack widths. Large, lightly reinforced beams showed wider cracks relative to smaller beams with the same amount of longitudinal reinforcement [4]. Lesley & Julio [34] carried out a series of experiments and saw a reduction in shear strength with increasing effective depth. Moreover, Sherwood, et al. [9] reported that in members without shear reinforcement and without distributed longitudinal reinforcement, the crack spacing at mid depth is proportional to member depth confirming the effect of depth on shear strength of RC beams.

2. Provisions for shear in beams without shear reinforcement in codes of practice

American Code (ACI 318–19)

V_c for non-prestressed members.

For sections with $A_v < A_{v,min}$,

$$V_c = [8\lambda_s\lambda(\rho_w)^{\frac{1}{3}}\sqrt{f_c'} + \frac{N_u}{6A_g}]b_w d \quad (\text{in} - \text{lb}) \tag{1}$$

$$V_c = [0.66\lambda_s\lambda(\rho_w)^{\frac{1}{3}}\sqrt{f'_c} + 0.037\frac{N_u}{A_g}]b_w d \quad (\text{mm} - \text{N}) \tag{2}$$

Where: V_c = Nominal shear strength provided by concrete A_g = Gross area of the concrete section b_w = Width of the section d = Effective shear depth of the member $f_c^{'}$ = Specified compressive strength of concrete ρ_w = Longitudinal tensile steel ratio N_u = Axial load acting on critical section.

Note that axial load, N_u is positive for compression and negative for tension. V_c shall be in the range of 0 and $5\lambda\sqrt{f_c'}b_w d$ (in-lb). The value of $\frac{N_u}{6A_g}$ shall not be taken greater than $0.05\sqrt{f_c'}$ (in-lb).

Size effect modification factor, λ_s, shall be determined by,

$$\lambda_s = \sqrt{\frac{2}{(1+\frac{d}{10})}} \quad (\text{in} - \text{lb}) \tag{3}$$

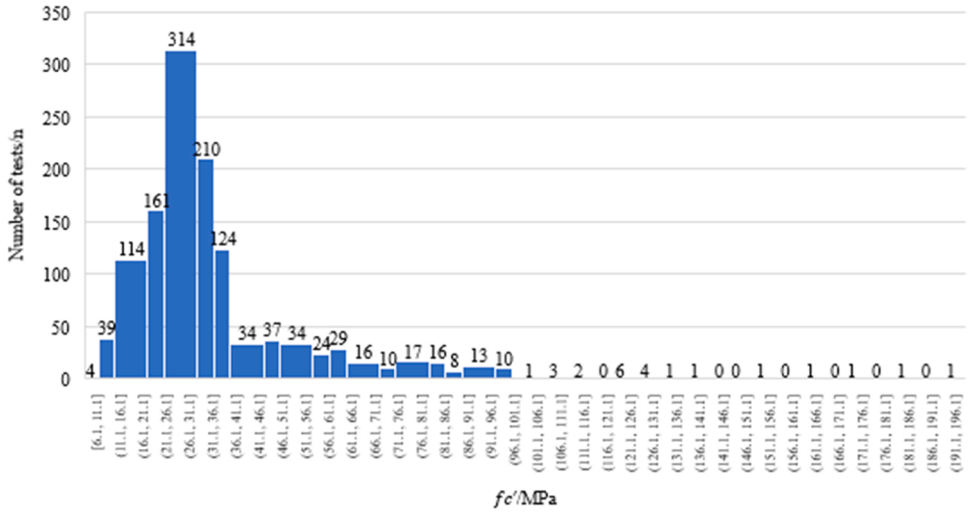

Fig. 2. $f_c^{'}$ variation in database (1 MPa = 145 psi).

$$\lambda_s = \sqrt{\frac{2}{1+\frac{d}{254}}} \quad (\text{mm}-\text{N}) \tag{4}$$

Australian Code (AS 3600–2018)

$$V_{uc} = k_v b_v d_v \sqrt{f_c'} \quad (\text{mm}-\text{N}) \tag{5}$$

Where:$f_c^{'}$ = Characteristic compressive (cylinder) strength of concrete at 28 days ($\sqrt{f_c^{'}} < 8$ MPa (1160 psi)).b_v = Width of the sectiond_v = Effective shear depth of the memberDetermination of the $k_v$and θ_v,

For a section with at least minimum shear reinforcement.

$$k_v = (\frac{0.4}{1+1500\varepsilon_x})(\frac{1300}{1000+k_{dg}d_v}) \tag{6}$$

Where,

I. $f_c^{'} \leq 65$ MPa (9427 psi) and not light-weight concrete

$$k_{dg} = [\frac{32}{(16+d_g)}] \tag{7}$$

II. $f_c^{'} > 65$ MPa (9427 psi) or light-weight concrete

$$k_{dg} = 2.0 \tag{8}$$

Determination of the longitudinal strain in concrete ϵ_x,

$$\varepsilon_x = \frac{\left|\frac{M^*}{d_v}\right| + |V^*| - P_v + 0.5N^* - A_{pt}f_{po}}{2(E_sA_{st}+E_pA_{pt})} \quad (\text{mm}-\text{N}) \tag{9}$$

Where,M= Moment at critical sectionV^*= Shear force at critical sectionN^*= Axial force at critical sectionA_{st}= Amount of tensile reinforcementA_{pt}= Amount of prestressing tendonsf_{po}= Stress in prestressing tendonsP_v= Shear force due to inclined prestressing tendons.

The angle of inclination of the concrete compression strut to the longitudinal axis of the member (θ_v) shall be calculated as follows:

$$\theta_v = (29+7000\varepsilon_x) \tag{10}$$

3. Development and characteristics of the database of past experimental results

A database which contains the results of 1237 shear tests carried out from 1948 to 2020 on point loaded RC beams without shear

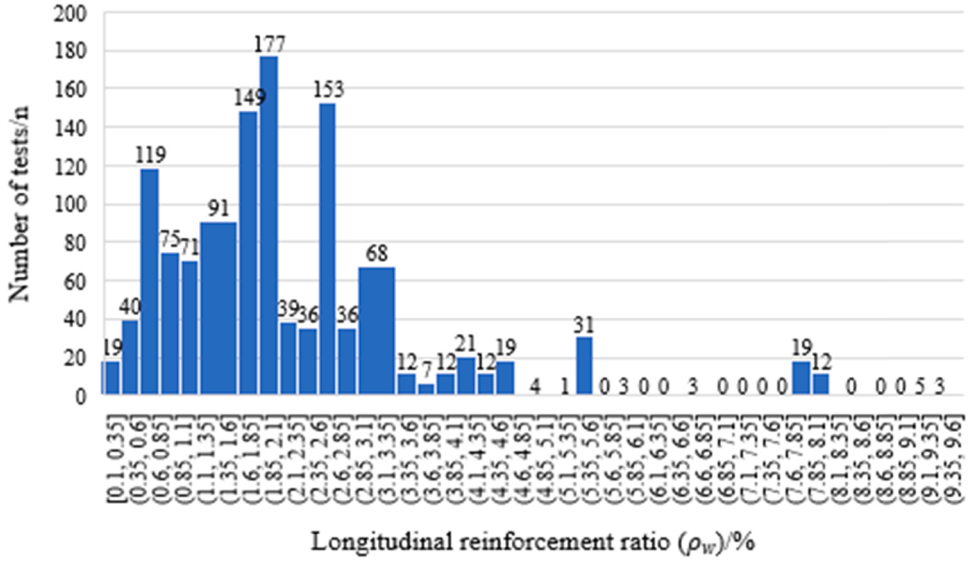

Fig. 3. ρ_w variation in database.

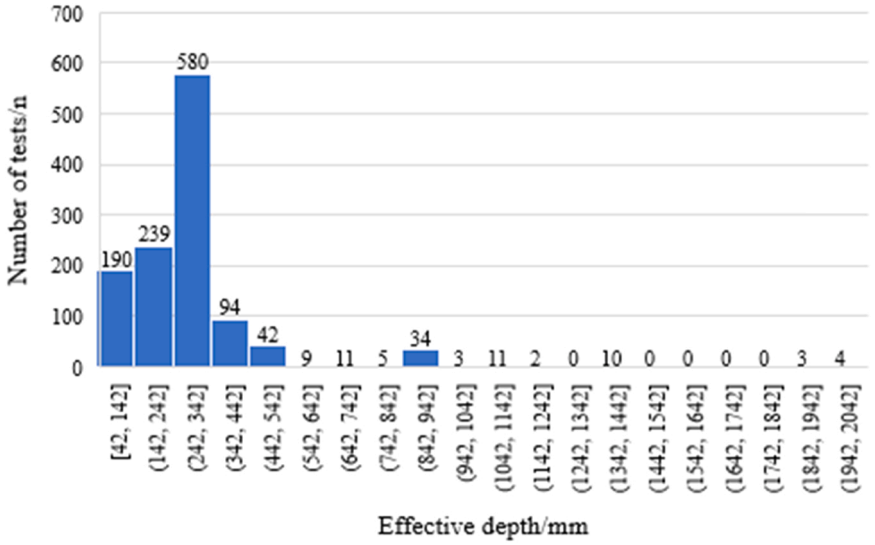

Fig. 4. Effective depth (d) variation in database (1 mm = 0.039 in).

reinforcement, was developed. Sherwood et.al [3] assembled 1849 test results (containing all types of beams, i.e. a/d < 2.5 and a/d > 2.5) using 114 references which contribute to more than 90% of test results for the database developed in this study. Evan & Buckley [35] pointed out that failure shear stresses of size effect experiments presented in Bažant & Kazemi [36] were 31–70% less than the results of repeating tests conducted by Evan C & Buckley. Thus, test results of Bažant & Kazemi [36] were not considered in this study. In addition to the database of Sherwood, et al. [3], six references were also considered for collecting shear failure data from research carried out between 2007 and 2018 [28,34,37–39]. Also note that, this database only consists of beams with point loads. All beam tests with uniformly distributed loads were not considered and beams with a/d < 2.5 were also not considered because the scope of this study is limited to slender beams.

In Fig. 2, the number of tests is plotted against $f_c^{'}$ with class intervals of $\Delta f_c^{'}$= 5 MPa (725 psi). The majority (75%) of the test data which amounts to 923 tests were reported for beams with $f_c^{'}$ between 16 MPa (2320 psi) and 41 MPa (5946 psi). In this study, all the tests with $f_c^{'}$ greater than 65 MPa (9427 psi) were considered as high strength concrete, corresponding to where ACI 318–19, CSA A23.3–04 and AS 3600–2018 limit the use of shear provisions. According to the histogram in Fig. 2, a relatively few tests (113) were performed on beams with high strength concrete (HSC).

The longitudinal reinforcement ratio ($\rho_w = \frac{A_s}{b_w d}$) is another key test parameter and has been considered in most of the design

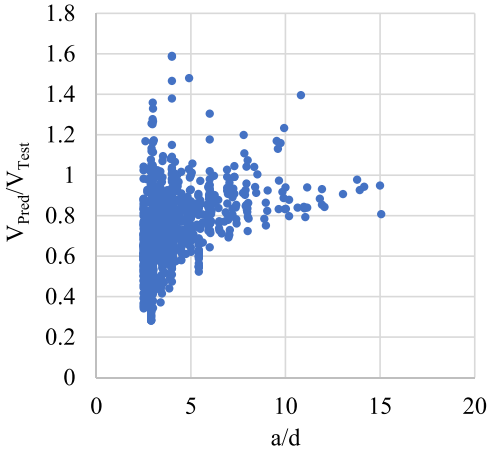

Fig. 5. Variation of the V_{Pred}/V_{Test} ratio with a/d.

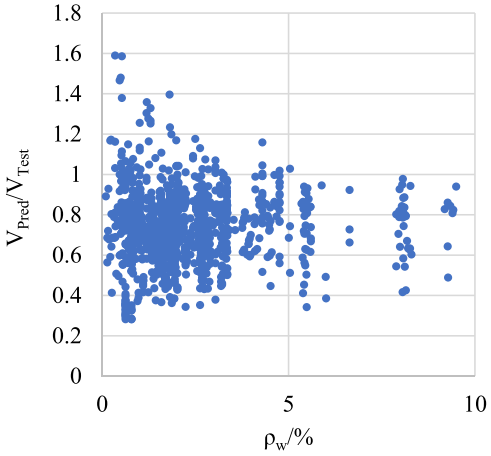

Fig. 6. Variation of the V_{Pred}/V_{Test}, ratio with ρ_w.

formulae that appear in design codes. In Fig. 3, the number of tests is plotted against ρ_w with class intervals of $\Delta\rho_w = 0.25\%$. Approximately 496 (41%) beams contained a reinforcement ratio of $\rho_w > 2\%$ and 253 (20%) beams contained a very low amount of ρ_w ($\rho_w < 1\%$). Further, 488 (39%) beams had reinforcement ratio between $1\% < \rho_w < 2\%$, representing what is most commonly used in practice.

As far as effective depth is concerned, Fig. 4 shows that the peak of 580 (47%) test beams were in the range between 242 mm (9.44 in) to 342 mm (13.38 in). Approximately 430 (35%) beams were reported with effective depth less than 242 mm (9.84 in) whereas only 30 (3%) beams had a high effective depth of $d > 1042$ mm (39.37 in).

4. Accuracy of shear provisions for slender beams without shear reinforcement

4.1. ACI 318–19

In the revised version of ACI 318, the one-way beam shear equation for non-prestressed concrete has been altered completely in order to account for the size effect and ρ_w [40]. According to previous investigations [1,3–9], lightly reinforced members experienced lower shear strength in which ACI 318–14 overestimated the shear strength. Size effect, which is found to be one of the most influential parameters [41], is considered. Particularly, for members with effective depths greater than 254 mm (10 in), the predicted shear strength is reduced by the size effect factor depending on effective depth of the beam. The attached appendix A in Jayasinghe et al. [1] shows calculation of shear strength according to Eq. (2). Fig. 5 depicts the variation of V_{Pred}/V_{Test} ratio with a/d ratio. An increase in the accuracy of the shear predictions can be seen, except for a few data points above 1 in beams with a/d ratio between 2.5 and 6. As a result of the strength reduction factor, all unconservative data points fall under 1. Overall, these failures result in an average V_{Pred}/V_{Test} of 0.76 with a coefficient of variation of 19% which measures the scatter of the predictions. The latest equation presented in ACI 318–19 [10] includes the ρ_w to the power of 1/3. Previous studies [42,43], which had performed regression analysis of experimental

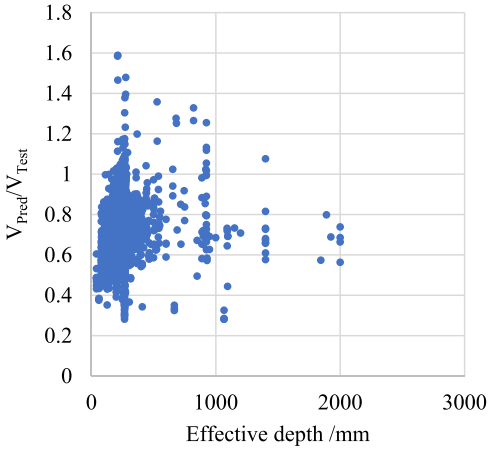

Fig. 7. Variation of the V_{Pred}/V_{Test} ratio with d. (1 mm = 0.039 in).

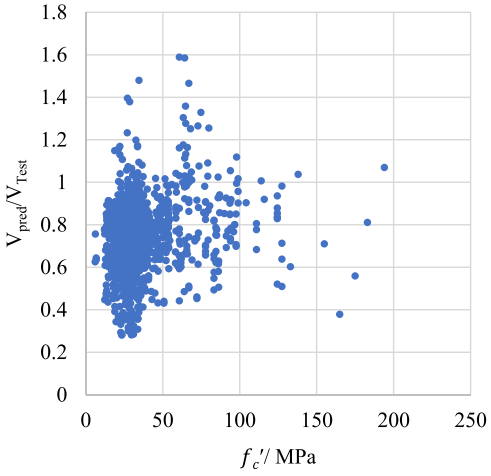

Fig. 8. Variation of the V_{Pred}/V_{Test} ratio with $f_c^{'}$. (1 MPa = 145 psi).

results, stated that shear response of an RC beam is proportional to $\rho_w{}^{1/3}$. Therefore, as shown in Fig. 6, a much-improved correlation with experimental results can be seen with the latest equation in ACI 318–19 especially with low ρ_w except for a few data points. Moreover, the predicted shear strengths of highly reinforced members show an improvement being closer to 1.

Fig. 7 depicts variation of V_{Pred}/V_{Test} against the effective depth of beams. The introduction of the size effect factor into the new one-way shear strength equation appears to have achieved a noticeable improvement in predicting the shear failure load of deeper beams, especially for effective depths greater than 1000 mm (40 in). As suggested in Bažant, et al. [44], this reflects the significance of the size effect factor in predicting shear failure load. The size effect factor in the new equation is based on the proposal of Bažant, et al. [44] and further reviewed in Yu, et al. [41]. Note that for beams without shear reinforcement, the size effect is neglected if the effective depth of the beam is less than 254 mm (10 in). Further, if the beam is provided with at least the minimum shear reinforcement amount, the size effect can be neglected unless the effective depth is greater than 2540 mm (100 in).

The new design approach in ACI 318–19 and other codes limit the contribution of high strength concrete to shear strength. ACI 318–19 limits the concrete strength to 69 MPa (10,000 psi), unless the member is provided with minimum shear reinforcement. The new equation and all other design approaches rely on the fact that the shear failure load is proportional to $\sqrt{f_c'}$, where noticeably no factor was considered to reflect the brittle behaviour of high strength concrete. As shown in Fig. 8, the ratio of V_{Pred}/V_{Test} beams with concrete strengths less than 60 MPa (8700 psi) are less than 1 except few data points. However, in beams with strengths between 60 MPa (8700 psi) and 100 MPa (14,500 psi), the shear failure loads are overestimated by a maximum factor of 1.6. Thus, it is observed that the shear capacity reduction with high strength concrete is still a cause for concern in predicting shear failure load.

Fig. 9 summarises the combined effect of effective depth and ρ_w on experimental nominal shear strength and how the new one-way shear equation predicts their influence. As the depth of the member increases, experimental shear strength decreases in all three ρ_ws being consistent with the conclusions of Kani [6] and Angelakos, et al. [4]. Fig. 9 also shows evidence that the proposed size effect term into the one-way shear approach works well with all three ranges of effective depths. As far as the effect of ρ_w is concerned, the lowest

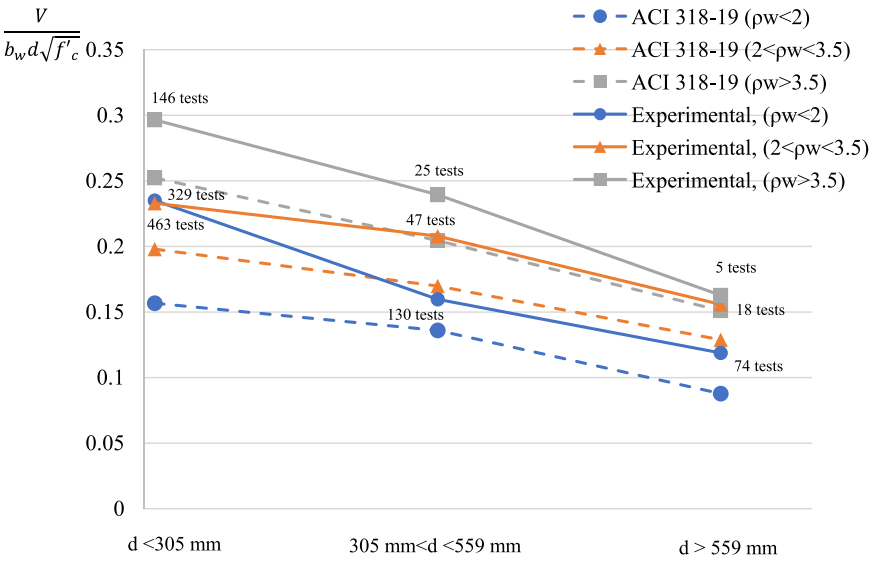

Fig. 9. Variation of the Normalized shear stresses with d and ρ_w. (1 mm = 0.039 in).

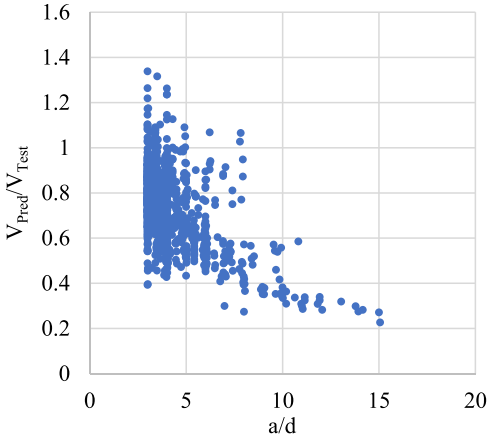

Fig. 10. Variation of the V_{Pred}/V_{Test} ratio with a/d.

observed nominal shear strengths are found in the beams with the lowest ρ_w. The introduction of the $\rho_w^{1/3}$ term has been successful in predicting shear response as it can capture the reduction of shear strength in lightly reinforced members. Moreover, for shallow beams (d < 305 mm (12 in)), shear strengths are slightly conservative compared to that of beams having moderate depths (305 mm (12 in) < d < 559 mm (22 in)) and larger depths (d > 559 mm (22 in)).

4.2. AS 3600–2018

Fig. 10 shows the shear response of AS 3600–2018 with variation of the a/d ratio. It must be noted that all predicted shear strengths are exclusive of the strength reduction factor ($\varnothing = 0.75$). It can be seen that as the a/d ratio decreases, the V_{Pred}/V_{test} ratio increases. Thus, it is possible that beams with a/d between 3 and 4 can be subjected to overestimation of shear strength. However, the inclusion of strength reduction factor appears to have mitigated the possibility of unsafe results. The average value of V_{Pred}/V_{Test} is 0.81 with a coefficient of variation of 16%. Furthermore, the conservatism continues to increase with increasing a/d ratio.

Simplified MCFT of Bentz, et al. [12] incorporates a size effect factor to their solution procedure in order to compensate for the influence of crack spacing. In AS 3600–2018, the second term of the k_v factor ($1300/1000 + k_{dg}d_v$) represents the so called size effect factor. It must also be noted that for RC beams with transverse reinforcement, the shear response is independent of the size effect factor [12]. Fig. 11 demonstrates how AS 3600–2018 treats the influence of the effective depth on predicted response of RC beams. It can be seen that AS 3600 predictions are reasonably consistent with shear failure results except for a few beams with effective depths between 200 mm and 500 mm. Thus, it is observed here that the inclusion of the size effect factor makes it possible to handle the influence of effective depth.

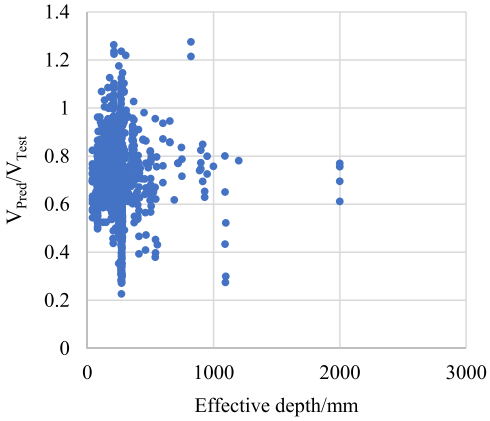

Fig. 11. Variation of the V_{Pred}/V_{Test} ratio with d. (1 mm = 0.039 in).

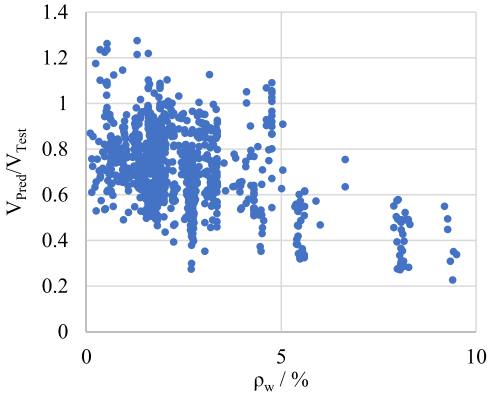

Fig. 12. Variation of the V_{Pred}/V_{Test} ratio with ρ_w.

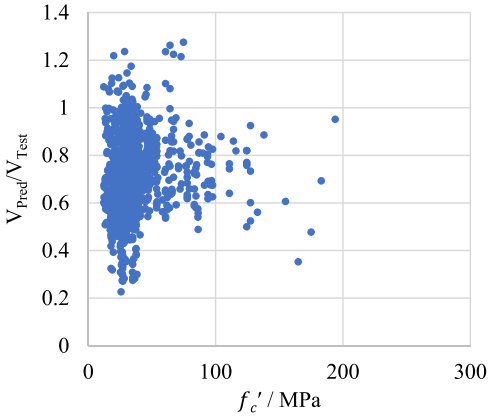

Fig. 13. Variation of the V_{Pred}/V_{Test} ratio with $f_c^{'}$. (1 MPa = 145 psi).

Tensile strain in longitudinal reinforcement is one of the main parameters which govern diagonal cracking strength of RC beams without shear reinforcement [3,7]. Tensile strain in longitudinal reinforcement is inversely proportional to ρ_w. When tensile strain in longitudinal reinforcement increases the diagonal crack width also increases, which leads to the breakdown of the aggregate interlock. Simplified MCFT [12] and AS 3600–2018 [17] introduced a strain effect factor that can account for the tensile strain in longitudinal reinforcement and ρ_w. In the AS 3600–2018 solution procedure, the first term of the k_v factor $(0.4/1 + 1500\varepsilon_x)$ represents the so-called strain effect factor. Therefore, AS 3600–2018 comprehensively accounts for the variation of longitudinal strain and ρ_w, resulting in consistent shear predictions as shown in Fig. 12. In fact, higher longitudinal reinforcement ratios which used to avoid flexural failures

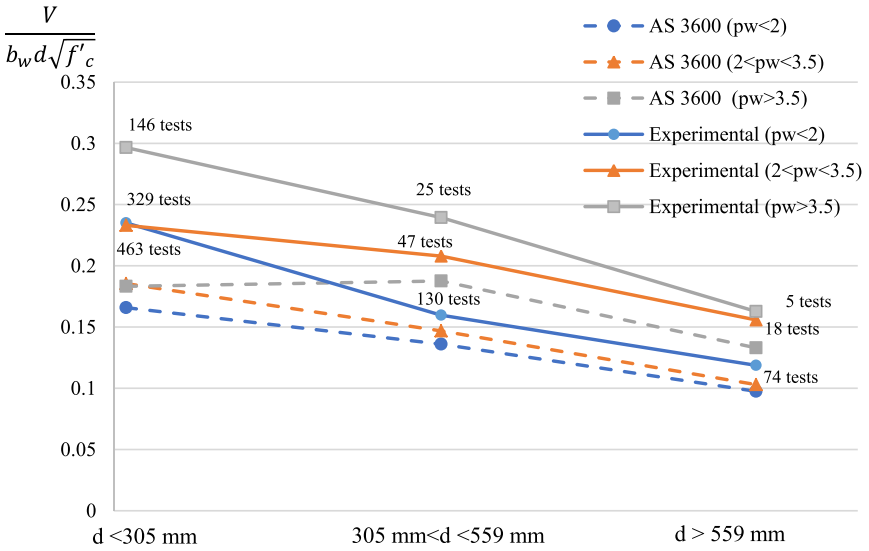

Fig. 14. Variation of the Normalized shear stresses with d and ρ_w. (1 mm = 0.039 in).

in tested beams have created extremely conservative predictions of shear strengths.

As far as the concrete compressive strength is concerned, AS 3600–2018 and CSA A23.3–04 impose a maximum value of design compressive strength of concrete: i.e., f'_c cannot exceed 65 MPa (9400 psi). As per these codes of practice, shear response is independent of the compressive strength of concrete for high strength concrete (f'_c > 65 MPa (9400 psi)) members. When the ductility of the concrete coincides with or exceeds that of the aggregate, the fracture goes through the aggregate resulting in a relatively smooth crack surface [28]. As mentioned before, it effectively incapacitates the aggregate interlock action. Thus, simplified MCFT has come up with a solution to compensate for this behaviour. As such, the recommendation in both AS 3600–2018 and CSA A23.3–04, where if f'_c > 65 MPa (9400 psi), the maximum aggregate size is considered to be zero. Fig. 13 shows the predicted shear response against the variation of f'_c. It can be observed that most of the data points have obtained V_{Pred}/V_{Test} less than 1. All points are less than 1.4 which indicates that inclusion of strength reduction factor can make all data point safe. Thus, AS 3600–2018 can safely predict the shear response of beams with f'_c up to 180 MPa (26,100 psi).

The same systematic analysis of combinations of factors explained previously is presented herein to further elaborate on the shear response of AS 3600. Fig. 14 summarises the combined effect of effective depth and $\rho_w$on the predicted response of AS 3600–2018.

It can be seen that as the effective depth increases the observed nominal shear strength ($\frac{V_{Test}}{b_w d\sqrt{f'_c}}$) decreases and the shear design procedure in AS 3600 – 2018 is capable of capturing that variation. Moreover, beams with lower ρ_w (ρ_w < 2) show a lower shear capacity whereas the predicted response follows the same pattern except for slight differences in beam with d < 305 mm (12 in). It is noted here that the calculated shear strengths of beams having intermediate ρ_w (2 < ρ_w < 3.5) explicitly follow the same trend of experimental results. Shallow beams (d < 305 mm (12 in)) with higher longitudinal reinforcement ratios experience an underestimation of shear strengths while beams with effective depths greater than 305 mm (12 in) show relatively consistent shear predictions with shear failure load.

5. Development of the artificial neural network (ANN)

5.1. Introduction to ANN

An ANN is, by definition, an interconnected network in which inputs and outputs are joined through connecting elements called neurons. The main computational characteristics of a neural network are their ability to learn functional relationships from examples and to discover patterns and regularities in data through self-organization. Over the last two decades, several studies were conducted to predict the shear strength of reinforced concrete elements using ANNs. Mansour et al. [45] developed an ANN and tested and trained against 176 of RC beams with shear reinforcement. Goh [46] investigated the feasibility of using neural networks to evaluate the ultimate strength of deep reinforced concrete beams subjected to shear and concluded that the neural network predictions were more reliable than the predictions of conventional equations. Sanad and Saka [47] also explored the use of ANN techniques in predicting the ultimate shear strength of reinforced concrete deep beams using 111 of deep beam tests. Cladera and Mari [43,48] employed ANNs to predict the shear strength of normal and high strength concrete beams with and without shear reinforcement. Cladera and Mari also developed new expressions for beams with and without shear reinforcement based on a parametric study conducted using ANNs [43, 48]. Oreta [49] conducted size effect study on shear strength of RC beams without shear reinforcement using an ANN. Further, Jung et al. [50] and Seleemah [51] investigated the applicability of ANNs for RC beams without shear reinforcement. ANNs have also been

Table 2
Ranges of input variables in the dataset.

Input	Training set		Validation set		Test set		Total set	
	Min	Max	Min	Max	Min	Max	Min	Max
d (mm)	80	1200	80	1097	80	1097	80	1200
d/b	0.2	7.08	0.2	7.09	0.2	7.21	0.2	7.21
ρ_w (%)	0.14	6.64	0.42	5.01	0.33	4.22	0.14	6.64
$f_c^{'}$ (MPa)	12.2	194	14.9	104.2	12.4	127.5	12.2	194
a/d	3	8.52	3	6.99	3	6.91	3	8.52

successfully used to predicted shear capacity of FRP reinforced concrete beams and steel-fibre reinforced concrete beams. Le et al. [52] predicted the axial load capacity of concrete-filled steel tube columns using ANN and observed that accuracy of ANN was superior to the current code equations. Asteris et al. [53] also developed novel hybrid predictive model combining balancing composite motion optimization and artificial neural network to predict the ultimate axial load of rectangular concrete-filled steel tubes. Armaghani et al. [54] applied ANN for the prediction of the unconfined compressive strength of granite using non-destructive texts. ANNs have further been used to predict other properties of concrete such as compressive strength [55], tensile strength [56] and has also been used in structural damage assessment [57,58].

Multi-layer Back-propagation neural networks (MBNN) are the most widely used type of ANNs in structural engineering application [46]. Goh [46] and Sanad and Saka [47] used BPNNs to predict the shear strength of deep beams and show that ANN performance is better than other existing formulae. Asteris et al. [59] implemented ANN approach to predict shear strength of reinforced concrete beams with shear reinforcement and highlighted that ANN is a trustworthy and effective method to evaluate the shear capacity. Armaghani et al. [60] employed feed forward ANN to predict shear strength of reinforced concrete beams and highlighted that $f_c^{'}$, a/d, effective span to effective depth (L/d), ρ_w and amount of shear reinforcement are the most influential parameters. Moreover, only few ANN studies have provided the final values of weights and biases which can be very useful for practicing engineers to produce an equation [61–63].

A back-propagation network usually starts with a random value for weights which connects layers of the ANN. The relationship between inputs and outputs is nonlinear, thus, nonlinear activation functions are employed for mapping the inputs with output. The "sigmoid function" and its variations are the most widely used activation functions in solving structural engineering problems [43,48]. In this study, Eq. (11) is employed as sigmoid function where x is calculated as shown in Eq. (12). In Eq. (12), n, w_i, b_i and *Input* are the number of input variables, weight matrix, bias vector and normalized input variables.

$$f(x) = \frac{1}{(1+e^{-x})} \tag{11}$$

$$x = \sum_{i=1}^{n}(w_i * Input + b_i) \tag{12}$$

The differences between the target and output of the ANN provide the training error. The weights are iteratively updated based on the gradient decent method [64] until the preassigned tolerance is satisfied or until the preassigned number of iterations is reached.

5.1.1. Data selection

The most important step in developing an ANN model for predicting shear strength is the collection of a suitable data set which represents a decent cross-section of the experimental test results. The completeness of the database is vital for the development of an effective ANN model. Only 645 shear test data was considered for the ANN, where results for beams with effective depth and width lower than 100 mm were not considered and results for beams with a/d ratio less 3 was also removed from the initial database presented in Section 5.3. Moreover, results for beams with effective depth of greater than 1200 mm were also removed as very limited number of tests were performed on these specimens. The minimum and maximum values of the input parameters of the database can be found in Table 2.

5.1.2. Input layer

The input layer of an ANN must receive inputs from the outside world. Too many input parameters can drastically slow down the learning process but, the accuracy of the trained function will be higher. However, for beams without shear reinforcement, input parameters can easily be identified or can be referred from the codes of practice.

The input parameters considered for the developed ANN are,

I. the effective depth (d)
II. the web slenderness factor d/b, where b is the web width
III. the a/d ratio
IV. the reinforcement ratio of longitudinal tensile steel (ρ_w), and
V. the compressive strength of concrete ($f_c^{'}$).

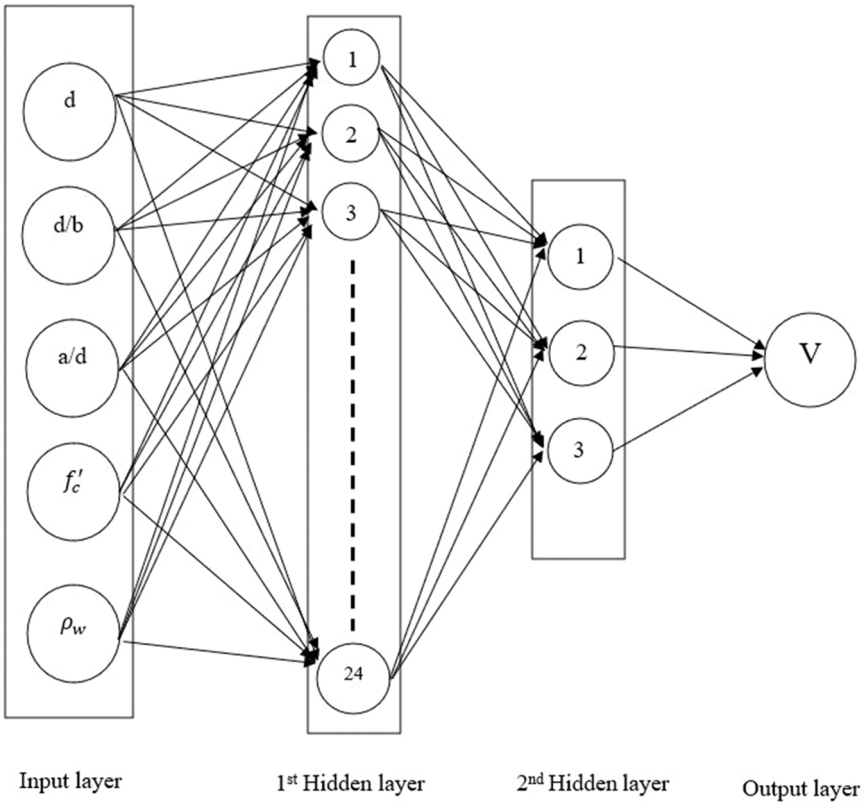

Fig. 15. Architecture of the ANN.

The output value is the failure shear strength of beams (V).

5.1.3. Hidden layer

A hidden layer is located between the input and the output layers of the ANN. This hidden layer applies weights to the inputs and directs them through the activation function. It also extracts and remembers useful information from the input layer. The number of hidden layers and the number of neurons in a hidden layer is determined by a process of trial-and-error. Lower hidden layers will not be able to capture the true behaviour of the function and too many hidden neurons will result in over-fitting. Over-fitting can produce false features between inputs and outputs producing unsuccessful predictions if the data has some noise. In this study, ANNs with one and two hidden layers were considered for the trail-and-error procedure.

5.1.4. Output layer

The output layer of the neural network produces the results of the ANN. In the problem analysed in this study the only output is the failure shear strength of RC beams without shear reinforcement, while an output layer of an ANN could have many outputs.

5.1.5. Normalisation of Input and output

Scaling of input and output data is very important because the activation function used in this study i.e., Sigmoid function, constraints the output to lie within the range (0,1). Therefore, scaling the input to the range of (−1,1) explicitly increases the learning speed, because these values fall into the region of the sigmoid function where the output is more sensitive to the variations of input values. In this study, a simple linear normalisation function was used as shown in Eq. (13).

$$Input = -1.0 + 2\frac{X - X_l}{X_u - X_l} \tag{13}$$

Where X is the unnormalised input, and X_l and X_u denote the lower and upper bounds of input variables.

Usually, a linear transformation is adequate for output parameters, although a nonlinear transformation is usually recommended if the data is clustered as in the case in this study. Therefore, the output parameters are first transformed using the following function,

$$S = \ln V \tag{14}$$

Where, V denotes the output value and ln is the Napier logarithm.

Table 3
Comparison of the 9 ANN architectures with statistical parameters.

ANN architecture	MAE		RMSE		R^2	
	Training	Validation	Training	Validation	Training	Validation
5.5.1	7.440	11.568	13.121	23.268	0.980	0.971
5.10.1	11.227	8.805	20.736	13.006	0.968	0.965
5.20.1	10.374	13.588	19.133	25.675	0.975	0.949
5.28.1	6.086	7.074	9.671	11.688	0.986	0.974
5.24.3.1	4.1772	6.958	6.310	9.464	0.991	0.984
5.26.5.1	3.810	8.146	5.322	13.275	0.991	0.983
5.25.8.1	3.230	7.526	4.601	12.235	0.993	0.982
5.28.21.1	2.548	12.563	3.760	17.264	0.995	0.945
5.29.30.1	1.985	10.184	3.313	18.756	0.997	0.956

After transforming according to Eq. (13), the output was normalised within the values of 0.1 and 0.9 for the sigmoid function as shown below:

$$Output = 0.1 + 0.8 * \frac{S - \ln(V_l)}{\ln(V_u) - \ln(V_l)} \tag{15}$$

Where, V_l and V_u denote the minimum and maximum values of the output variable.

5.1.6. Architecture of the ANN

A trial-and-error procedure was used to determine the optimum architecture for the ANN. A number of inputs and output were initially fixed. Further, the leaning rate and momentum parameters were kept unchanged at 0.4 and 0.1, respectively. Proper determination of the number of neurons in a hidden layer is to some extend problem-specific in predicting shear capacity of RC beams. For instance, Oreta [49], Cladera and Mari [43] and Mansour et al.[45] developed ANNs with one hidden layer and Jung and Kim [65] and Lee and Lee [66] developed ANNs with two hidden layers. Thus, in this study, both options were considered, and ANN with the optimum architecture was obtained considering the lowest RMSE. Fig. 15 shows the optimum architecture for the developed ANN based on the trial-and-error discussed in Section 5.3. Furthermore, final value of weights and biases are given as supplementary material. Thus, other researchers and practicing engineers can produce same ANN architecture and can be used to develop an equation to predict shear strength of beams without shear reinforcement.

5.2. Performance of the ANN

The ANN model developed in this study is used to predict the shear strength of 645 RC beams without shear reinforcement. As previously mentioned, the training set was used to develop the ANN including weights and biases associated with each neuron and it is also used to optimize the weights and biases of each neuron. Testing set is never used to train the ANN. However, the ANN was capable of generalising the relationship between the input variables and the output variables and reasonable performance was seen as shown in Fig. 17.

The performance of the ANN was evaluated using several statistical indicators such as mean absolute error (MAE), root mean square error (RMSE) and determination of coefficient (R^2). The mathematical expressions for these are presented as follows,

$$RMSE = \sqrt{\frac{\sum_{i=1}^{n} (V_{Predict} - V_{Exp})^2}{n}} \tag{16}$$

$$MAE = \frac{\sum_{i=1}^{n} |V_{Predict} - V_{Exp}|}{n} \tag{17}$$

$$R^2 = 1 - \frac{\sum_{i=1}^{n} (V_{Exp} - V_{Predict})^2}{\sum_{i=1}^{n} (V_{Exp} - \overline{V}_{Predict})^2} \tag{18}$$

Where; V_{Exp} is the experimental shear strength of beams, $V_{Predict}$ is the predicted shear strength using ANN, $\overline{V}_{Predict}$ is the mean of the predicted shear strengths and n indicated the number of samples.

As described in Table 3, nine ANN structures were evaluated against these statistical parameters. Four ANN structures with one hidden layer and five ANN structures with two hidden layers were considered. Lower values of MAE and RMSE and values near 1 for R^2 demonstrate the higher accuracy of the ANN architecture. As observed, increasing the number of hidden layers and the number of neurons in a hidden layer significantly enhanced the performance of the training set. However, increasing the number of hidden layers

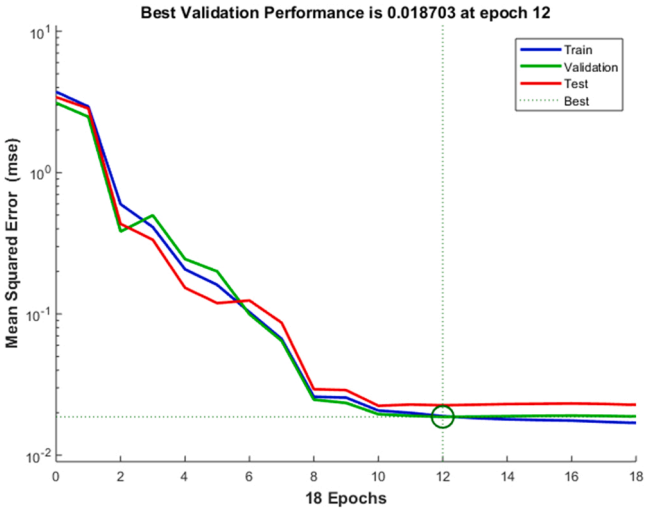

Fig. 16. Performance of the ANN with respect to MSE.

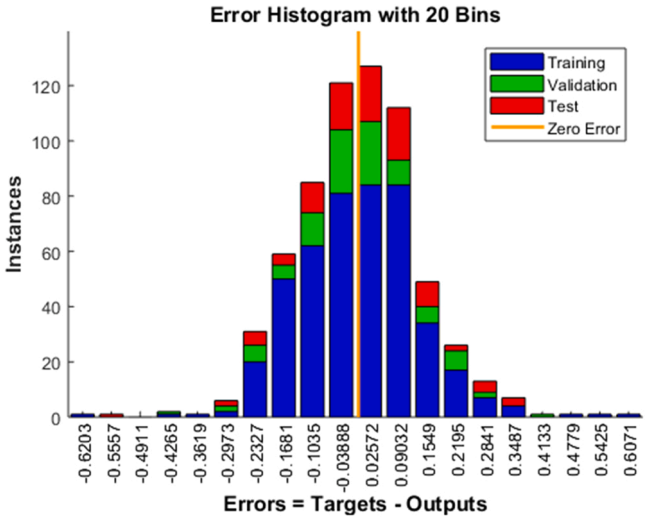

Fig. 17. Error histogram from MATLAB analysis.

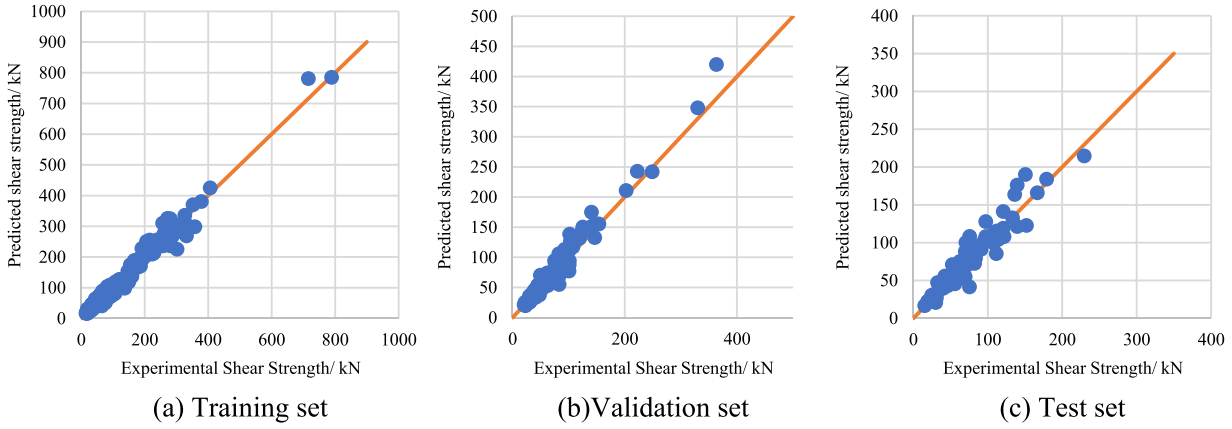

Fig. 18. Comparison between predicted shear failure load using the ANN and experimental load against (a) training, (b) validation and (c) test sets.

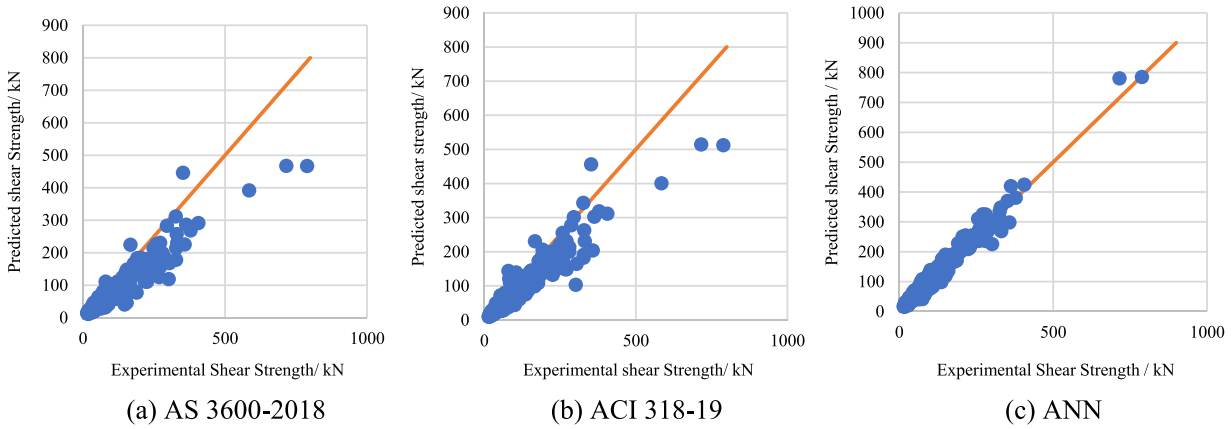

Fig. 19. Comparison of predicted shear failure load and experimental shear failure load according to (a) AS 3600–2018, (b) ACI 318–19 and (c) ANN.

Table 4
Comparison of ANN predictions with ACI 318–19 and AS 3600–2018 shear strength predictions.

	Mean ($\frac{V_{Exp}}{V_{Pred}}$)	Stdev	CoV
AS 3600–2018	1.378	0.294	0.213
ACI 318–19	1.352	0.256	0.189
ANN (Training set)	1.005	0.122	0.122
ANN (Validation set)	0.992	0.136	0.137
ANN (Test set)	1.002	0.164	0.164
ANN (All)	1.002	0.131	0.131

Stdev=Standard deviation, CoV= Coefficient of variation

and neurons in a hidden layer exacerbate the possibility of overfitting. As seen in Table 3, increasing the number of neurons in a hidden layer does not explicitly enhance the ANN performance against the validation set. Therefore, choosing an optimum ANN architecture is vital to obtain better performance with ANN. As noted in Table 2, the ANN architecture 5.24.3.1 showed better performance for both training set and validation set, thus, this ANN structure was chosen to predict the shear strength of RC beams without shear reinforcement. Fig. 16 and Fig. 17 demonstrate the performance of the ANN considering MSE against training, validation and test sets and error histogram obtained from MATLAB, respectively. Fig. 18 (a), (b) and (c) illustrate the performance of the ANN against the training set, the validation set and the testing set.

The comparison of the experimental shear strength and predicted shear strength by ANN algorithm and code equations are given in Fig. 19 and the ratio of the experimental shear strength to the ANN predicted strength is given in Table 4. The average value of this ratio for ANN is 1.005 and coefficient of variation is 12%, which are comparably lower than the AS 3600–2018 and ACI 318–19. According to Fig. 19 and Table 4, the ANN was successful in predicting shear strengths compared to ACI 318–19 and AS 3600–2018.

5.3. Parametric analysis based on the ANN results

The parametric study performed in Section 4 demonstrated that the considered variables are interdependent. Thus, a clear trend between variables and failure shear force cannot be established. Further, a very few experimental tests were conducted isolating the effect of a single variable on the shear failure load of RC beams without shear reinforcement. Thus, an ANN is an effective tool to investigate the influence of each variable individually.

5.3.1. Influence of the effective depth (d)

As mentioned previously, the effective depth and size effect is paramount to the shear failure strength of beams without shear reinforcement. In fact, size effect on the shear capacity of RC beams without shear reinforcement depends on the compressive strength of concrete. ANN was used for a set of virtual input variables with different effective depths while keeping other variables constant. Other variables including longitudinal reinforcement ratio and a/d ratio were kept constant at 3% and 3 respectively.

As seen in Fig. 20, increasing effective depth of the beams reduces the shear strength. As discussed previously, the effective depth of the beam influences crack widths of the critical shear crack. Large, lightly reinforced beams showed wider cracks relative to smaller beams with the same amount of longitudinal reinforcement. In fact, the effect of the effective depth on shear failure strength increases with increasing compressive strength of concrete. Increasing concrete strength increases the probability of aggregate fracturing on the shear crack further exacerbating the shear transfer through aggregate interlock which was already being incapacitated due to large

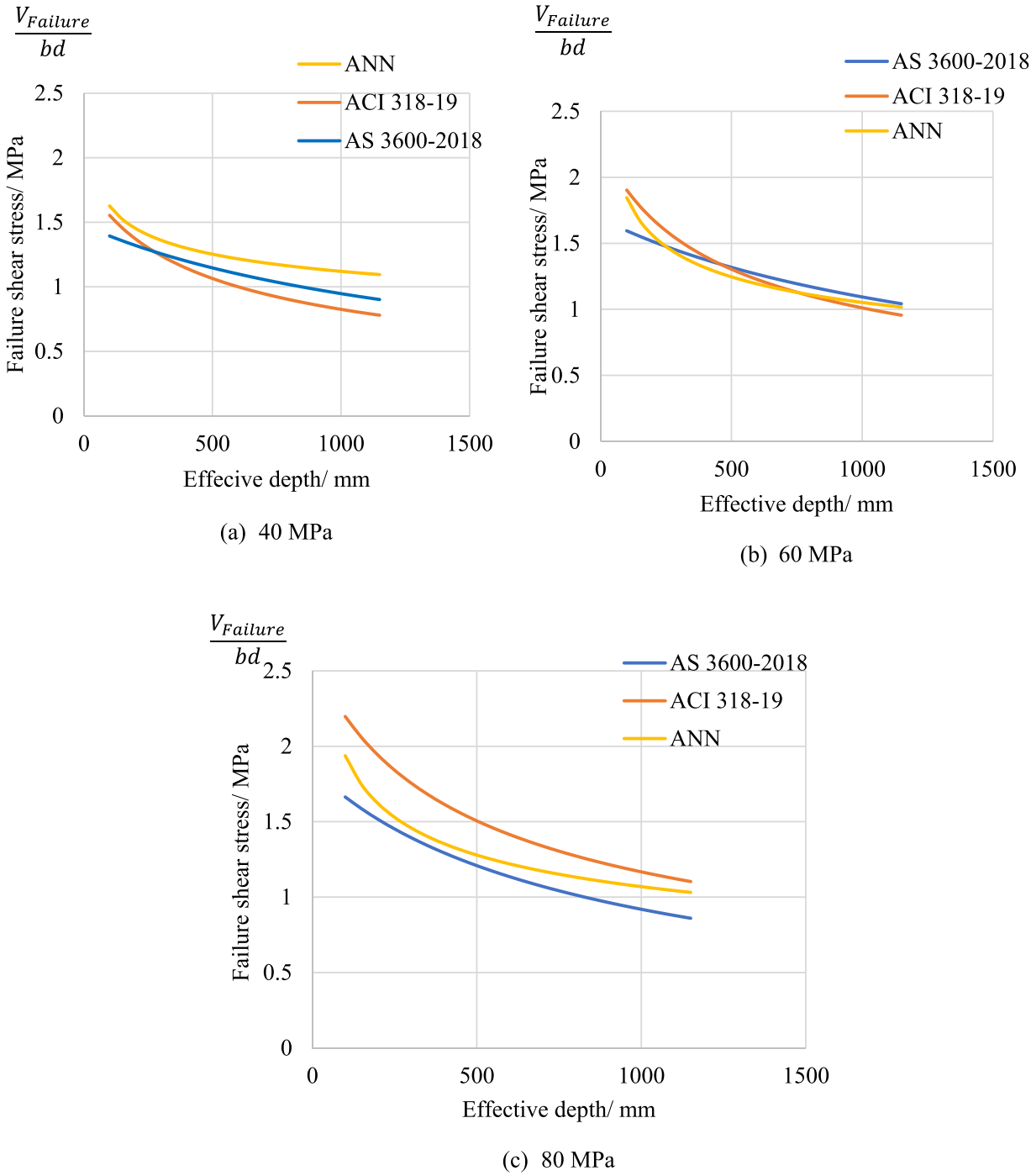

Fig. 20. Variation of shear strength against effective depth of beams three different concrete strengths (a) 40 MPa, (b) 60 MPa and (c) 80 MPa.

crack widths in larger beams.

5.3.2. Influence of the compressive

5.3.2.1. strength of concrete, $f_c^{'}$. Fig. 21 shows the failure shear strength of RC beams without shear reinforcement as a function of compressive strength of concrete. Other variables including, effective depth, longitudinal reinforcement ratio, d/b ratio and a/d ratio were kept constant at 600 mm, 3%, 1.5 and 3 respectively. As observed, the effect of concrete strength on shear failure strength of RC

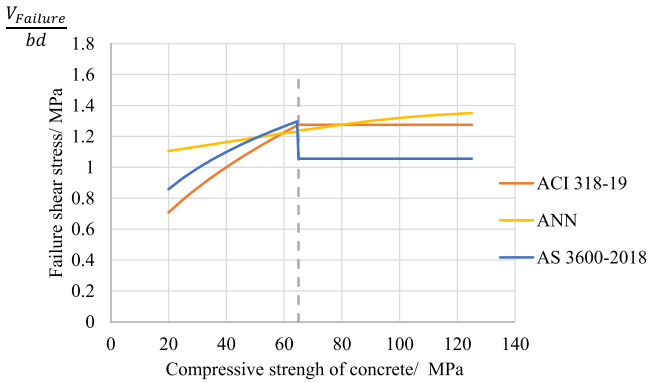

Fig. 21. Variation of failure shear strength with compressive strength of concrete ($f_c^{'}$).

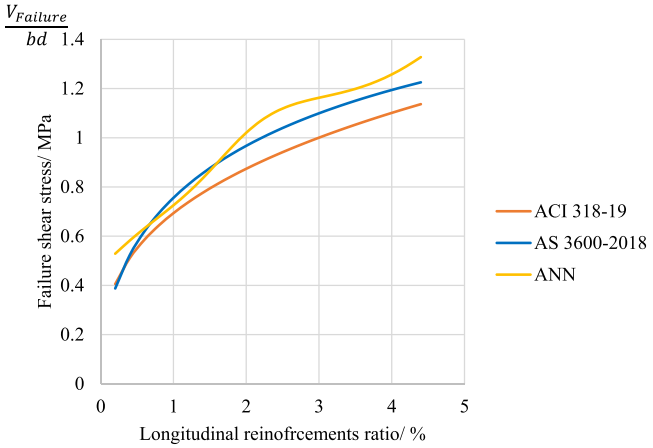

Fig. 22. Variation of failure shear strength against longitudinal reinforcement ratio.

beams without shear reinforcement is very minimal. As discussed earlier, higher the concrete strength the more susceptible the member is to aggregate fracturing causing reduced aggregate interlock. As observed, after 65 MPa, the predicted shear failure stress according to AS 3600–2018 was abruptly reduced because for concrete strengths greater than 65 MPa, the code recommends $k_{dg} = 2$ which denotes the zero-aggregate size. This assumption in AS 3600–2018 of zero aggregate size after 65 MPa results in the zero-shear stress transfer due to aggregate interlock. Shear predictions of both ACI 318–19 and AS 3600–2018 do not depend on the compressive strength of concrete for values of compressive strength greater than 65 MPa.

5.3.3. *Influence of the amount of longitudinal reinforcement*

Fig. 22 depicts the variation of failure shear strength as a function of longitudinal reinforcement ratio according to the ACI 318–19, AS 3600–2018 and the developed ANN. As described early, a low longitudinal reinforcement ratio reduces the shear capacity because a low amount of longitudinal reinforcement increases the longitudinal strain in the concrete which subsequently increase the crack width resulting in lower aggregate interlock stress transfer along the critical shear crack. Both ACI 318–19 and AS 3600–2018 have reasonably captured the effect of longitudinal reinforcement ratio on shear strength. As observed, the ANN prediction was also appreciably comparable to predictions of the ACI 318–19 and AS 3600–2018 predictions except for slight deviation at higher longitudinal reinforcement ratios. Therefore, it can be determined that the ${\rho_w}^{1/3}$ term in ACI 318–19 reasonably captured the effect of longitudinal reinforcement ratio on shear strength of RC beams without shear reinforcement. Also, the strain effect factor in AS 3600–2018, explicitly considers the influence of ρ_w on shear strength of RC beams without shear reinforcement.

5.3.4. *Influence of the a/d ratio*

The variation of failure shear strength with a/d ratios are shown in Fig. 23. ACI 318–19 dose not account for the effect of a/d on shear strength of RC beams without shear reinforcement. However, as seen in Fig. 23, AS 3600–2018 predictions are influenced by a/d ratios. Moreover, variations resulting from ANN show consistency with the AS 3600–2018 results highlighting the importance of a/d ratio's influence on the failure shear strength of beams without shear reinforcement. According to the ANN predictions, lower a/d demonstrated higher shear failure strength while higher a/d ratios reduced the shear strength. In fact, this observation can be due to

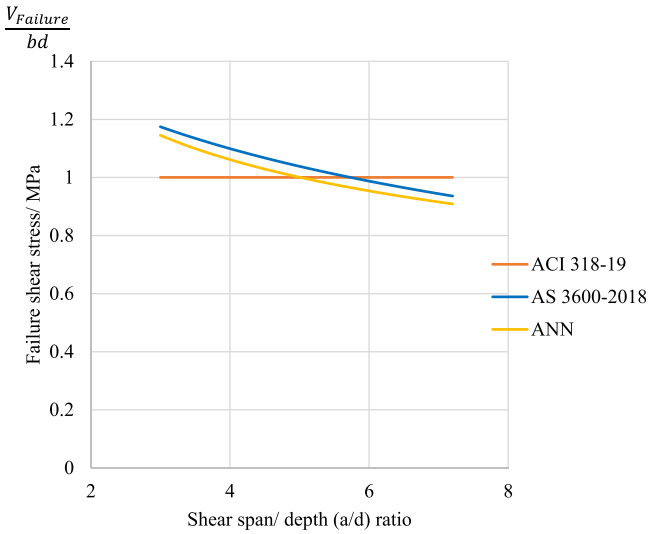

Fig. 23. Variation of failure shear strength against shear span to depth (a/d) ratio.

the influence of truss action in beams with lower a/d ratio. Influence of direct truss action enhances the post-cracking shear strength of the beams where beams with high a/d ratios fail after the development of the critical shear crack.

6. Conclusions

In this study, a comprehensive parametric study was carried out using a database of 1237 shear failure results of slender beams without transverse shear reinforcement subjected to point loads. The study was carried out evaluating two sectional shear design procedures presented in ACI 318–19 and AS 3600–2018. Using a subset with 645 beam test data of the initial database, an ANN model was developed to predict the shear strength of RC beams without shear reinforcement. The following conclusions were drawn from this study:

1. The new one-way shear design equation proposed in ACI 318–19 exhibited appreciable accuracy in predicting the shear failure load. The proposed size effect factor works well with deeper members achieving comparable accuracy with SMCFT. Although, a longitudinal strain-based factor is not proposed, a relatively consistent shear prediction can be seen with the $\rho_w^{1/3}$ term.
2. The recently updated AS 3600–2018 showed relatively consistent shear predictions with the database of 1237 beam shear failures. While being another adaptation of simplified MCFT, it could achieve safe shear predictions. It was found that the strain effect and size effect factors could explicitly capture the impact of strain in longitudinal reinforcement and member depth respectively. Moreover, in the context of high strength concrete beams, assuming zero aggregate size provided safe predictions.
3. An ANN model with 5 input variables i.e., the effective depth (d); the web slenderness factor d/b, where b is the web width; the a/d ratio; the reinforcement ratio of longitudinal tensile steel (ρ_w); and the concrete compressive strength ($f_c^{'}$) was developed. The optimum architecture of the ANN was obtained based on the lowest RMSE and ANN with 24 and 3 neurons in 1st and 2nd hidden layers demonstrated the most optimum performance against both training and validation set. Accuracy of the ANN was observed to be notably higher than the predictions of the ACI 318–19 and AS 3600–2018 against the referred experimental data.
4. Using the trained ANN model, a parametric study was conducted to investigate the variation of the shear failure stress against the effective depth (d); the reinforcement ratio of longitudinal tensile steel (ρ_w); the concrete compressive strength ($f_c^{'}$) and shear span to depth ratio (a/d). The influence of effective depth of beams on shear failure stress was comparable among equations from codes of practice and the ANN. Moreover, ANN and codes were able to capture the influence of ρ_w on the shear failure stress. Compressive strength of concrete on shear failure has very limited influence for high strength concrete. Shear span to depth ratio has significant impact on shear failure stress although ACI 318–19 did not take into account its influence.

Declaration of Competing Interest

The authors declare the following financial interests/personal relationships which may be considered as potential competing interests: Thushara Jayasinghe reports article publishing charges was provided by The University of Melbourne. Priyan Mendis reports a relationship with The University of Melbourne that includes: funding grants.

Acknowledgements

This research was funded by the Cooperative Research Centres Project 8 Grant CRCPEIGHT000084: Upcycling solutions for hazardous claddings and co-mingled waste and authors would like to acknowledge the Faculty of Engineering and Information Technology, The University of Melbourne for supporting with the Graduate Research Scholarship.

References

[1] T. Jayasinghe, T. Gunawardena, P. Mendis, A comparative study on minimum shear reinforcement provisions in codes of practice for reinforced concrete beams, Case Stud. Constr. Mater. 15 (2021), e00617.
[2] ACIC. Building Code Requirements for Structural Concrete (ACI 318–14) and Commentary (318R-14). Farmington Hills, Mich: American Concrete Institute; 2014.
[3] E.G. Sherwood, C.B. Evan, P.C. Michael, Where is shear reinforcement required? Review of research results and design procedures, Acids Struct. J. (2008) 590–600.
[4] D. Angelakos, E.C. Bentz, M.P. Colliins, Effect of concrete strength and minimum stirrups on shear strength of large members, Acids Struct. J. 98 (3) (2001) 290–300.
[5] M.P. Collins, D. Kuchma, How safe are our large, lightly reinforced concrete beams, slabs, and footings? Acids Struct. J. (1999) 482–490.
[6] G.N.J. Kani, Basic facts concerning shear failure, ACI J. 63 (6) (1966) 675–692.
[7] G.N.J. Kani, How safe are our large reinforced concrete beams? ACI J. 64 (3) (1967) 128–141.
[8] B.A. Podgorniak-Stanik, The influence of concrete strength, distribution of longitudinal reinforcement, amount of transverse reinforcement and member size on shear strength of reinforced concrete members, Tor. Grad. Dep. Civ. Eng., Univ. Tor. (1998).
[9] E.G. Sherwood, A.S. Lubell, E.C. Bentz, M.P. Collins, One-way shear strength of thick slabs and wide beams, Acids Struct. J. 103 (6) (2006) 794–802.
[10] ACI C.. Building Code Requirements for Structural Concrete (ACI 318–19). Farmington Hills: American Concrete Institute; 2019.
[11] F.J. Vecchio, M.P. Collins, The modified compression field theory for reinforced concrete elements subjected to shear, ACI J. 83 (2) (1986) 219–231.
[12] E.C. Bentz, F.J. Vecchio, M.P. Collins, Simplified modified compression field theory for calculating shear strength of reinforced concrete elements, Acids Struct. J. 103 (4) (2006) 614–624.
[13] F.J. Vecchio, M.P. Collins, Predicting the response of reinforced concrete beams subjected to shear using modified compression field theory, Acids Struct. J. 85 (1988) 258–268.
[14] A23.3 CC. Design of Concrete Structures. Mississauga, ON, Canada: Canadian Standards Association; 2004.
[15] CEB-FIB. fib Model Code for Concrete Structures 2010. Germany: Fib - Federation Internationale Du Beton; 2010.
[16] AASHTO. LRFD Bridge Design Specifications and Commentary. Washington, DC,: American Association of State Highway and Transportation Officials; 1994.
[17] 3600–2018 A. Concrete Structures. Sydney: Standards Australia; 2018.
[18] F. Cavagnis, J.T. Simões, M.F. Ruiz, A. Muttoni, Shear strength of members without transverse reinforcement based on development of critical shear crack, Acids Struct. J. 117 (2020) 1.
[19] Y. Yang, J. den Uijl, J. Walraven, Critical shear displacement theory: on the way to extending the scope of shear design and assessment for members without shear reinforcement, Struct. Concr. 17 (5) (2016) 790–798.
[20] M.P. Collins, E.C. Bentz, E.G. Sherwood, Where is shear reinforcement required? Review of research results and design procedures, Acids Struct. J. 105 (5) (2008) 590–600.
[21] R.C. Fenwick, T. Paulay, Mechanisms of shear resistance of concrete beams, J. Struct. Div. ASCE 94 (ST10) (1968) 2325–2350.
[22] Morsch E. Der Eisenbetonbau (Reinforced Concrete Construction). Stuttgart, Germany: Verlag von Konrad Witwer; 1922.
[23] Mihaylov B. Behaviour of Deep Reinforced Concrete Beams under Monotonic and Reversed Cyclic Load. Thesis Submitted in Partial Fulfilment of the Requirements for the Degree of Doctor of Philosophy in EARTHQUAKE ENGINEERING. European School for Advanced Studies in Reduction of Seismic Risk, ROSE SCHOOL; 2008.
[24] R. Taylor, R.S. Brewer, The effect of the type of aggregate on the diagonal cracking of reinforced concrete beams, Mag. Concr. Res. 115 (44) (1963) 87–92.
[25] R.S. Pendyala, P. Mendis, Experimental study on shear strength of high-strength concrete beams, Acids Struct. J. 97 (4) (2000) 564–571.
[26] M. Fujita, R. Sato, K. Matsumoto, Y. Takaki, Size effect on shear strength of RC beams using HSC without shear reinforcement, Transl. Proc. JSCE 56 (711) (2002) 113–128.
[27] M.K. Johnson, J.A. Ramirez, Minimum shear reinforcement in beams with higher strength concrete, Acids Struct. J. 86 (4) (1989) 376–382.
[28] S. Perera, H. Mutsuyoshi, Shear behavior of reinforced high-strength concrete beams, Acids Struct. J. 110 (2013) 1.
[29] A.H. Elzanaty, A.H. Nilson, F.O. Slate, Shear capacity of reinforced concrete beams using high-strength concrete ACI, Journal 83 (2) (1986) 290–296.
[30] J.G. MacGREGOR, p Gergely, Suggested revisions to ACI building code clauses dealing with shear in beams, Acids Struct. J. 74 (10) (1977) 493–500.
[31] E.I. Saqan, R.J. Frosch, Influence of flexural reinforcement on shear strength of prestressed concrete beams, Acids Struct. J. 106 (1) (2009) 60–68.
[32] D. Angelakos, The influence of concrete strength and longitudinal reinforcement ratio on the shear strength of large size reinforced concrete beams with and without, transverse reinforcement. Toronto, ON, Canada: Department of Civil Engineering, University of Toronto, 1999.
[33] B. Hu, Y.-F. Wu, Effect of shear span-to-depth ratio on shear strength components of RC beams, Eng. Struct. 168 (1) (2018) 770–783.
[34] H.S. Lesley, A.R. Julio, Influence of effective depth on shear strength of concrete beams—experimental study, Acids Struct. J. 107 (5) (2010) 554–562.
[35] C.B. Evan, S. Buckley, Repeating a classic set of experiments on size effect in shear of members without stirrups, Acids Struct. J. 102 (6) (2005) 832–838.
[36] Z.P. Baznt, M.T. Kazemi, Size effect on diagonal shear failure of beams without stirrups, Acids Struct. J. 88 (3) (1991) 268–276.
[37] G. Aguilar, S. Villamizar, A.R. Julio, Evaluation of shear reinforcement design limits in high-strength concrete beams, Acids Struct. J. 115 (2) (2018) 401–414.
[38] D. Daluga, K. McCain, M. Murray, S. Pujol, Effect of geometric scaling on shear strength of reinforced concrete beams without stirrups, Acids Struct. J. 115 (1) (2018) 5–14.
[39] Q. Deng, W.-J. Yi, F.-J. Tang, Effect of coarse aggregate size on shear behavior of beams without shear reinforcement, Acids Struct. J. 114 (5) (2017) 1131–1142.
[40] A.M. de Sousa, Mounir K. Lantsoght EOaED, One-way shear strength of wide reinforced concrete members without stirrups, Struct. Concr. 1 (2020) 23.
[41] Q. Yu, J.-L. Le, M.H. Hubler, R. Wendner, G. Cusatis, Z.P. Bazant, Comparison of main models for size effect on shear strength of reinforced and prestressed concrete beams, Struct. Concr. 17 (5) (2016) 778–789.
[42] S.H. Ahmad, A.R. Khaloo, A. Poveda, Shear capacity of reinforced high-strength concrete beams, ACI J. 83 (2) (1986) 297–305.
[43] A. Cladera, A. Marí, Shear design procedure for reinforced normal and high-strength concrete beams using artificial neural networks, Part I: Beams Stirrups. Eng. Struct. 26 (7) (2004) 917–926.
[44] Z.P. Bazant, Q. Yu, W. Gerstle, J. Hanson, W. Ju, Justification of ACI 446 proposal for updating ACI code provisions for shear design of reinforced concrete beams, Acids Struct. J. 104 (5) (2017) 601–610.
[45] M.Y. Mansour, M. Dicleli, J.-Y. Lee, J. Zhang, Predicting the shear strength of reinforced concrete beams using artificial neural networks, Eng. Struct. 26 (6) (2004) 781–799.
[46] A.T. Goh, Prediction of ultimate shear strength of deep beams using neural networks, Struct. J. 92 (1) (1995) 28–32.
[47] A. Sanad, M. Saka, Prediction of ultimate shear strength of reinforced-concrete deep beams using neural networks, J. Struct. Eng. 127 (7) (2001) 818–828.
[48] A. Cladera, A. Mari, Shear design procedure for reinforced normal and high-strength concrete beams using artificial neural networks. Part II: beams with stirrups, Eng. Struct. 26 (7) (2004) 927–936.
[49] A.W.C. Oreta, Simulating size effect on shear strength of RC beams without stirrups using neural networks, Eng. Struct. 26 (5) (2004) 681–691.

[50] S.-M. Jung, S.-E. Han, K.-S. Kim, Prediction of shear strength using artificial neural networks for reinforced concrete members without shear reinforcement, J. Comput. Struct. Eng. Inst. Korea 18 (2) (2005) 201–211.
[51] A.A. Seleemah, A neural network model for predicting maximum shear capacity of concrete beams without transverse reinforcement, Can. J. Civ. Eng. 32 (4) (2005) 644–657.
[52] T.-T. Le, P.G. Asteris, M.E. Lemonis, Prediction of axial load capacity of rectangular concrete-filled steel tube columns using machine learning techniques, Eng. Comput. (2021) 1–34.
[53] P.G. Asteris, M.E. Lemonis, T.-A. Nguyen, H. Van Le, B.T. Pham, Soft computing-based estimation of ultimate axial load of rectangular concrete-filled steel tubes, Steel Compos. Struct. 39 (4) (2021) 471–491.
[54] D.J. Armaghani, A. Mamou, C. Maraveas, P.C. Roussis, V.G. Siorikis, A.D. Skentou, et al., Predicting the unconfined compressive strength of granite using only two non-destructive test indexes, Geomech. Eng. 25 (2021) 317–330.
[55] H.-G. Ni, J.-Z. Wang, Prediction of compressive strength of concrete by neural networks, Cem. Concr. Res. 30 (8) (2000) 1245–1250.
[56] D.-K. Bui, T. Nguyen, J.-S. Chou, H. Nguyen-Xuan, T.D. Ngo, A modified firefly algorithm-artificial neural network expert system for predicting compressive and tensile strength of high-performance concrete, Constr. Build. Mater. 180 (2018) 320–333.
[57] X. Wu, J. Ghaboussi, J. Garrett Jr., Use of neural networks in detection of structural damage, Comput. Struct. 42 (4) (1992) 649–659.
[58] C.-B. Yun, J.-H. Yi, E.Y. Bahng, Joint damage assessment of framed structures using a neural networks technique, Eng. Struct. 23 (5) (2001) 425–435.
[59] P.G. Asteris, D.J. Armaghani, G.D. Hatzigeorgiou, C.G. Karayannis, K. Pilakoutas, Predicting the shear strength of reinforced concrete beams using Artificial Neural Networks, Comput. Concr. 24 (5) (2019) 469–488.
[60] D.J. Armaghani, G.D. Hatzigeorgiou, C. Karamani, A. Skentou, I. Zoumpoulaki, P.G. Asteris, Soft computing-based techniques for concrete beams shear strength, Procedia Struct. Integr. 17 (2019) 924–933.
[61] P.G. Asteris, V.G. Mokos, Concrete compressive strength using artificial neural networks, Neural Comput. Appl. 32 (15) (2020) 11807–11826.
[62] P.G. Asteris, A.D. Skentou, A. Bardhan, P. Samui, K. Pilakoutas, Predicting concrete compressive strength using hybrid ensembling of surrogate machine learning models, Cem. Concr. Res. 145 (2021), 106449.
[63] P.G. Asteris, P.B. Lourenço, M. Hajihassani, C.-E.N. Adami, M.E. Lemonis, A.D. Skentou, et al., Soft computing-based models for the prediction of masonry compressive strength, Eng. Struct. 248 (2021), 113276.
[64] J. Hertz, A. Krogh, R.G. Palmer, Introduction to the Theory of Neural Computation, CRC Press, 2018.
[65] S. Jung, K.S. Kim, Knowledge-based prediction of shear strength of concrete beams without shear reinforcement, Eng. Struct. 30 (6) (2008) 1515–1525.
[66] S. Lee, C. Lee, Prediction of shear strength of FRP-reinforced concrete flexural members without stirrups using artificial neural networks, Eng. Struct. 61 (2014) 99–112.